

Conceptual Design Optimization of Tensairity Girder Using Variable Complexity Modeling Method

Shi Yin* and Ming Zhu**

School of Aeronautic Science and Engineering, Beihang University, Beijing 100191, China

Haoquan Liang***

School of Automation Science and Electrical Engineering, Beihang University, Beijing 100191, China

Da Zhao****

School of Aeronautic Science and Engineering, Beihang University, Beijing 100191, China

Abstract

Tensairity girder is a light weight inflatable fabric structural concept which can be used in road emergency transportation. It uses low pressure air to stabilize compression elements against buckling. With the purpose of obtaining the comprehensive target of minimum deflection and weight under ultimate load, the cross-section and the inner pressure of tensairity girder was optimized in this paper. The Variable Complexity Modeling (VCM) method was used in this paper combining the Kriging approximate method with the Finite Element Analysis (FEA) method, which was implemented by ABAQUS. In the Kriging method, the sample points of the surrogate model were outlined by Design of Experiment (DOE) technique based on Optimal Latin Hypercube. The optimization framework was constructed in iSIGHT with a global optimization method, Multi-Island Genetic Algorithm (MIGA), followed by a local optimization method, Sequential Quadratic Program (SQP). The result of the optimization gives a prominent conceptual design of the tensairity girder, which approves the solution architecture of VCM is feasible and efficient. Furthermore, a useful trend of sensitivity between optimization variables and responses was performed to guide future design. It was proved that the inner pressure is the key parameter to balance the maximum Von Mises stress and deflection on tensairity girder, and the parameters of cross section impact the mass of tensairity girder obviously.

Key words: inflatable structures, optimization, surrogate model, variable complexity modeling

Nomenclature

r_1	Radius of beginning and end cross section
r_2	Radius of middle cross section
p	Inner pressure of airbeam
m	Mass of airbeam
σ_v	Maximum Von Mises stress of airbeam
u	Deflection of roller
f	Applied force from roller
l	Length of airbeam

1. Introduction

Inflatable fabric structures have been utilized in a variety of fields ranging from spacecraft antenna [1], solar sail [2], airship [3] to hovercraft [4] due to the high performance of lightweight, high level of reliability, easy-deployed, low cost, etc. With the requirement of rapid makeshift bridge in case of the pavement damage from disaster or war, here comes a kind of tensairity girder for light vehicles is proposed because of its distinct features of easy-built, portable and even housed

This is an Open Access article distributed under the terms of the Creative Commons Attribution Non-Commercial License (<http://creativecommons.org/licenses/by-nc/3.0/>) which permits unrestricted non-commercial use, distribution, and reproduction in any medium, provided the original work is properly cited.

© * Master candidate
** Associate professor
*** Postdoctoral, corresponding author: haoquan.liang@buaa.edu.cn
**** Master candidate

by an SUV.

A load bearing behavior of asymmetric spindle and cylinder shaped tensairity was studied experimentally under variant loads and compared to FEA [5,6,7]. The regularities of property of spindle shaped tensairity girder was investigated by changing the parameters including initial inner pressure, member cross section, membrane stiffness span-diameter ratio etc.[8]. The performance and sensibility of High altitude and long endurance airship was studied revealing the effects on the capability of airship payload, size and area required of solar cell with consideration of pressure difference, temperature difference, helium purity, seasons, operation altitude, wind speed etc.[3]. Also, the Variable Complexity Modeling (VCM) method was implemented in the optimization problem of the composite wing, in which the optima of the current surrogate model was used to update the sample points to decrease the weight of the wing [9].

As the researches above only focused on the load bearing behavior of tensairity girder and the VCM method for aircraft, this study builds an optimization architecture for the tensairity girder using the VCM method [10-13] to improve the validity of tensairity girder, which combines the surrogate approximate model with the nonlinear finite element analysis. The Kriging method [11,14,15] and adaptive sampling method [9] are used to build the surrogate model. The MIGA [16,17] is used to seek the global optima and the SQP method [18] is to find the local optimal during the optimization procedure.

2. Architecture of optimization

Equation Chapter (Next) Section 1

The purpose of the conceptual design optimization problem of the tensairity girder is to minimize the mass of the airbeam while minimizing the deflection of the airbeam. Therefore, this optimization problem is a multi-objective problem. In this paper, the multi-objective is scaled and weighted as Eq.(1) using the factors in Table 1

Table 1. Scalar and weighting factor for the multi-objective optimization problem

Parameter	Objective	Scalar factor	Weighting factor
<i>m</i>	minimize	10.0	0.5
<i>u</i>	minimize	0.05	0.5

Table 2. Range of variables

Design variables	Lower bound	Initial value	Upper bound
<i>r</i> ₁ [m]	0.150	0.245	0.340
<i>r</i> ₂ [m]	0.350	0.425	0.500
<i>p</i> [Pa]	30000	45000	60000

to take advantage of developed theory of single objective optimization.

$$Obj = \sum_{i=1}^n \frac{w(i) \times x(i)}{s(i)} \tag{1}$$

In Eq.(1), *w(i)* is the weighting factor and *s(i)* is the scalar factor. These two factors are initial value of each response variable [19].

In the conceptual design optimization problem of the tensairity girder, the design variables are the radius of the edge section *r*₁, the radius of the middle section *r*₂ and the inner pressure *p*. Refer to related conclusions and experiments, the range of variables is as

Table 2. The median value in the range is taken as initial value for optimization loop.

Accordingly, the mathematical description of the conceptual design optimization problem of the tensairity girder can be formulated as Eq.(2) and Eq.(3).

$$\min_{r_1, r_2, p} Obj = 0.5 \times \frac{m(r_1, r_2, p)}{10} + 0.5 \times \frac{u(r_1, r_2, p)}{0.05} \tag{2}$$

$$\begin{aligned} & \sigma_v \leq 5 \times 10^7 \\ \text{s.t.} \quad & 0.15 \leq r_1 \leq 0.34 \\ & 0.35 \leq r_2 \leq 0.50 \\ & 30000 \leq p \leq 60000 \end{aligned} \tag{3}$$

In response to the difficult in significant computational expense occurred in the high fidelity FEA during conventional optimization loop, the VCM method takes advantage of refined and computationally expensive model together with rational and computationally inexpensive model [11], namely, surrogate model. The VCM method runs an efficient way in computational complexity reduction but keeping analysis precision. While operating on computationally inexpensive model, the VCM method adjusts its precision by calling computationally expensive model periodically.

The framework of VCM optimization process contains three parts: global to local optima seeking based on surrogate

model, nonlinear FEA and update of sample points. The framework mainly operates approximate analysis based on surrogate model during the iteration of optimization, while the sample space of surrogate model is updated by FEA simultaneously in which the design variables are obtained by global to local optima seeking aforementioned. The surrogate model in the loop has been modified up to convergence.

For algorithms in the optimization framework, MIGA is employed to global optimization, which inherits genetic algorithm (GA) and improves it. Normally, GA fits well into engineering solution where discontinuities and multimodality may exit, because GA does not utilize derivative information [14]. Additionally, MIGA overcomes the premature of traditional GA and accelerates the process of convergence [16].

Accordingly, SQP is employed to local optimization. SQP fits the nonlinear problem with constraints well, because it's based on gradient optimization and has a hand at the exploration around initial design point. However, the drawback of SQP is the strong dependence on initial design point leading to converge to local optima early. So, in the frame of optimization, MIGA gives initial global optima to SQP as initial design point for getting real global optima that would solve the problem more efficiently [10,11].

In the architecture, the sample spaces of surrogate model in global optimization and local optimization are based on Optimal Latin Hypercube DOE. The process of the architecture is as below. Firstly, global optimization algorithm traverses the design space and outlines the sensitive area rapidly. Secondly, local optimization algorithm targets this area and searches it accurately to find out an initial optima. Then, design variables of the initial optima are sent to nonlinear FEA for getting precise optimal response values. At last, the design variables and the precise response values of initial optima above are added to sample space return to perform the optimization loop, the stop criteria of the loop is that each relative error

of the adjacent scaled multi-objective and the two response values is less than $10e-4$.

The iSIGHT framework and the flow chart of the optimization problem is illustrated as Fig. 1 and Fig. 2 respectively.

2.1 Initial sampling

The initial sample space contains 50 sample points of which variables are arrayed by Optimal Latin Hypercube DOE and responses are produced by FEA accordingly. Here, three design variables are input, three responses are output as well. The framework of DOE is as Fig. 3.

2.2 Surrogate model build

2.2.1 Creation: Kriging method

Kriging is a useful interpolation method for irregular data, it works excellently in unbiased estimation of regional

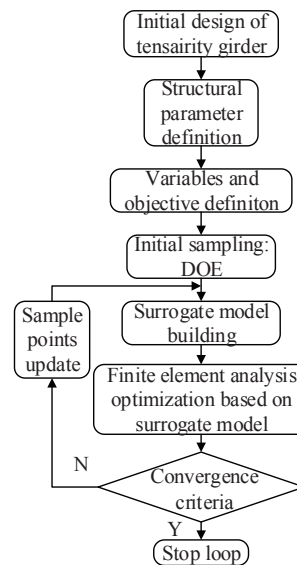


Fig. 2. Flow chart of iSIGHT framework of optimization

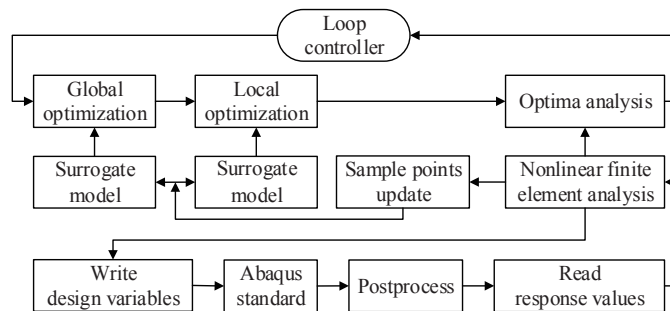


Fig. 1. iSIGHT framework of optimization

variable. In Kriging method, response $y(x)$ is the sample function of stochastic process $Y(x)$, based on reasonable assumption, the stochastic process contains regressive part and stochastic part.

$$Y(x) = \sum_{j=1}^k \beta_j f_j(x) + Z(x) = F^T(x)\beta + Z(x) \quad (4)$$

As Eq.(4), regressive part as well as the first term is that the average of stochastic process is estimated by linear combination of k preliminary functions; stochastic part as well as the second term is that the values of observation points are estimated more accurately by approximation function through the quantization of correlation between observation points and neighbour points.

By its nature, the Kriging is an algebraic expression which provides smooth derivative information. [11] The Kriging method does interpolation in DOE sample space to establish a reliable surrogate model. Although expensive to build initially, the method uses minimal resources once implemented. As the implementation proved the surrogate model is an efficient and appropriate substitute for FEA as it reduces CPU time dramatically.

2.2.2 Update: adaptive sampling method

The initial surrogate model is built based on initial sample space, then the optimization process works on the initial surrogate model and generates the initial optima that will be added to the sample space return. So, next

optimization process can work on an updated surrogate model, which will be more accurate in the repeat of the loop in Fig. 1. The flow chart of sample space updating is illustrated as Fig. 4.

3. Model for optimization

In the model, the wheel of vehicle is simulated by the roller to hit the tensairity girder as Fig. 5. And the parameters of tensairity girder are as Table 3. r_1 , r_2 and p are the design variables of the optimization problem, which is illustrated in Fig. 6, and the values in Table 3 are the initial ones during optimization process. The rest parameters in Table 3 are the fix ones regarding some papers and results of experiments related [5-8].

The model of the airbeam is carried out in ABAQUS/Standard version 13.0. The girder is suspended from ground by restriction on the head point, end point and the symmetrical plane. The middle main part of tensairity girder is modeled with a 4-node quadrilateral membrane with reduced integration and hourglass control (M3D4R), a 3-node triangular membrane (M3D3) is for the head and end part. The loading of the structure in the FEA process is done in three step: (1) pre-inflation of the airbeam with a lower inner pressure; (2) full inflation of the airbeam; (3) loading the force from roller with the finite sliding formulation of surface to surface contact.

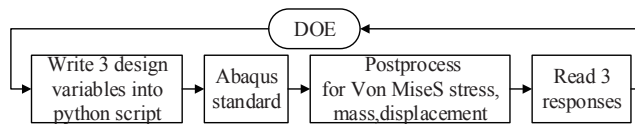


Fig. 3. Design of Experiment process

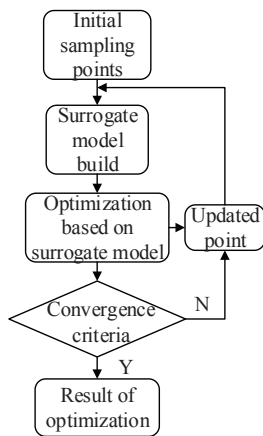


Fig. 4. The flow chart of sample space updating

Table 3. Parameters of airbeam

Parameters	Value
$r_1[m]$	0.245
$r_2[m]$	0.425
$l[m]$	5
$p[Pa]$	45000
$f[N]$	600
Young's modulus[GPa]	1
Poisson's ratio	0.45
density[Kg/m ³]	1400
failure load σ_b [MPa]	71
safety factor n	1.5
allowable stress $\sigma = \sigma_b/n$ [MPa]	50

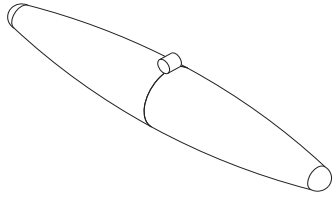


Fig. 5. Basic model

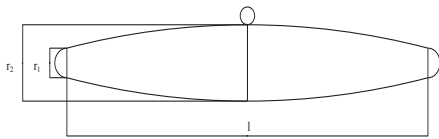


Fig. 6. parameter r_1, r_2, l in basic model

Table 4. The comparison between optimized result and baseline

Parameter	Baseline	Optimized value	Rate of change
$r_1[m]$	0.245	0.172	-29.691%
$r_2[m]$	0.425	0.436	2.564%
$p[Pa]$	45000	56524	25.609%
$m[Kg]$	20.778	11.110	-46.532%
$\sigma_v [Pa]$	2.546e7	1.665e7	-34.613%
$u[m]$	0.1002	0.0195	-80.533%

4. Results and comparison

The loop ran 46 iterations to meet the convergence criteria. As Table 4 and Fig. 7, the results give an outstanding optimization of 46% decrease in m , 34% decrease in σ_v and 80% decrease in u dramatically. The outline of optimization is illustrated as Fig. 8, compared to upper and lower bound. Fig. 9 and Fig. 10 show the Von Mises stress and deflection contour of the tensairity girder in the optimal design variable

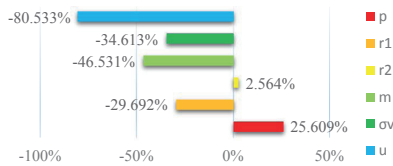


Fig. 7. Rate of change

under ultimate load produced by ABAQUS.

5. Sensitivity analysis

5.1 Single variable sensitivity analysis

Sensitivity analysis reveals the system sensitivity to the change of variables or parameters. It helps ascertain the influence on objective functions or constraint functions and the coupling between subsystems from the change of system variables or parameters. Also, the design of system, the direction of exploration, decision support are dependent on it [20].

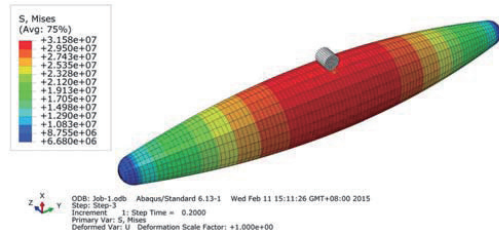


Fig. 9. The stress contour of σ_v

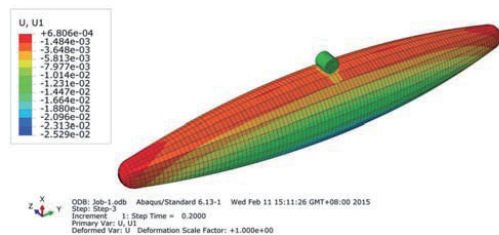


Fig. 10. The deflection contour of u

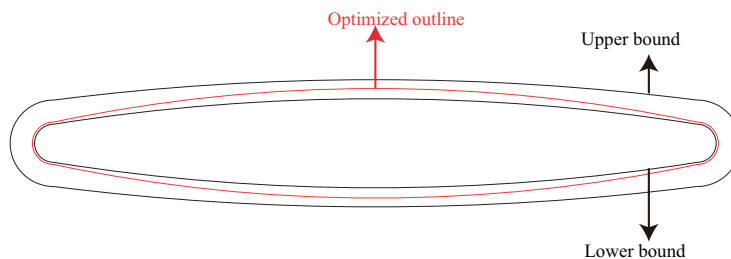


Fig. 8. Comparison of basic and optimized outline

5.1.1 Mass of airbeam sensitivity analysis

The mass of the airbeam is an important indicator because the portable and easy-built capacity are reliable on the lightweight. As Fig. 11, the mass of airbeam increases linearly with increase in the value of r_1 nearly, keeping other variables constant in optimal values. For a 10mm increase in r_1 results in approximately 1.7kg in airbeam mass. Similarly, it is found that the mass of airbeam increases linearly with increase in the value of r_2 nearly, keeping other variables constant in optimal values. For example, 100mm increases in r_2 results in approximately 1.9kg in airbeam mass. But the pressure does not affect the mass from the result. The tendency helps in the analysis.

5.1.2 Deflection of roller sensitivity analysis.

Deflection is another important indicator of tensairity girder, u is an appropriate one in this model. As Fig. 12, u decreases with the increases in inner pressure of airbeam, keeping other variables constant in optimal values. In linear regression analysis, the fitting precision is up to 0.9857. For a 10,000Pa increase in inner pressure results in about 3.5mm decrease in u . Also, u decreases nonlinearly with the increases in r_1 , keeping other variables constant in optimal values. In [150mm, 225mm], u decreases 3.25mm with a 50mm increase in r_1 , but the tendency is not obvious in [225mm, 340mm]. And, u decreases linearly with the increases in r_2 partly, keeping other variables constant in optimal values. For a 50mm increase in r_2 results in about 7.5mm decrease in u . The influence of r_2 is more obvious than r_1 .

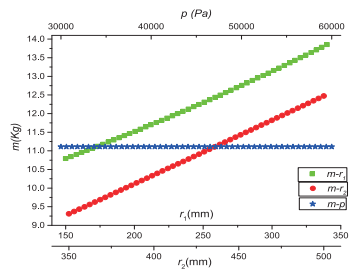


Fig. 11. Mass of airbeam sensitivity analysis

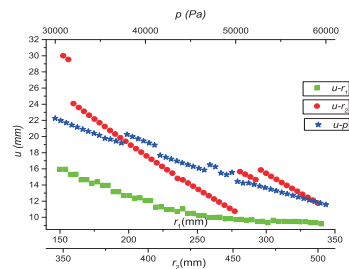


Fig. 12. Deflection of roller sensitivity analysis

5.1.3 Maximum Von Mises stress of airbeam sensitivity analysis

The third important indicator is the maximum σ_v of airbeam in this model. As Fig. 13, σ_v increases linearly with the increases in inner pressure, keeping other variables constant in optimal values.

For example, σ_v increases about 5.6MPa with a 10,000Pa increase in inner pressure. In regression analysis, the fitting precision is up to 0.9999. As well, σ_v increases with the increases in r_1 , keeping other variables constant in optimal values. In [150mm, 250mm], the tendency is nonlinear. But in [250mm, 340mm], a 50mm increase in r_1 results in about 0.2MPa increase in σ_v . Moreover, σ_v increases linearly with the increases in r_2 , keeping other variables constant in optimal values. For example, σ_v increases about 2MPa with a 50mm increase in r_2 . In regression analysis, the fitting precision is up to 0.9999. Compared to r_1 , r_2 has a significant impact on performance. That's why the curvature has a significant influence on the area stress where the loads act upon. That's a meaningful reference above.

5.2 Coupling sensitivity analysis.

Because r_1 and r_2 are both structural parameters, the analysis is based upon them, keeping inner pressure of airbeam optimized value. A quadratic regression analysis is conducted to reveal the relationship between the 3 responses and variables r_1 , r_2 , with Response Surface Methodology (RSM) using polynomial to fit design space.

As Fig. 14, there is the influence contribution rate to mass of airbeam, including first order, second order and coupling term in r_1 and r_2 . As follows, -0.4802% is to the coupling term,

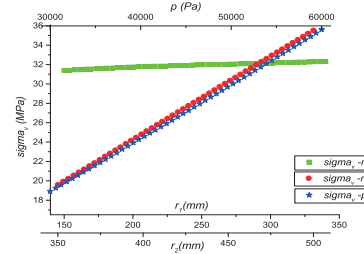


Fig. 13. Maximum Von Mises stress of airbeam sensitivity analysis

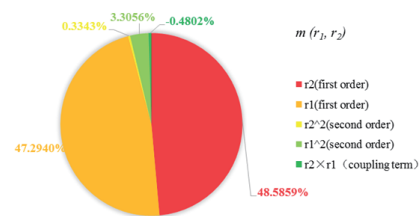


Fig. 14. Contribution rate in $m(r_1, r_2)$

namely, the influence of r_1 with r_2 on mass of airbeam can be ignored. The fitted design space of mass is shown in Fig. 15.

As Fig. 16, in the coupling sensitivity analysis of u , the rate of coupling term in r_1 and r_2 is -6.6705%, that can't be ignored as it's even bigger than the rate of second order in r_1 .

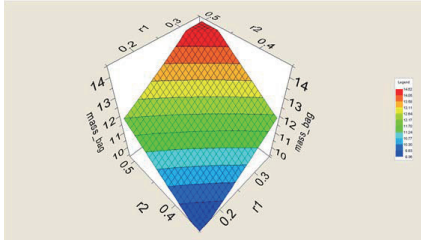


Fig. 15. Fitted design space of $m(r_1, r_2)$

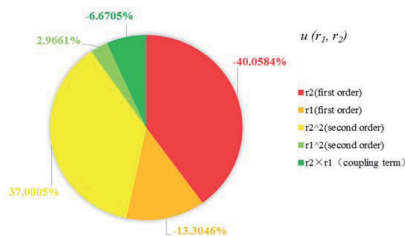


Fig. 16. Contribution rate in $u(r_1, r_2)$

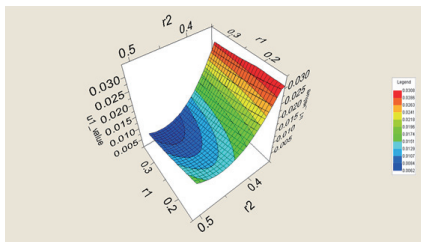


Fig. 17. Fitted design space of $u(r_1, r_2)$

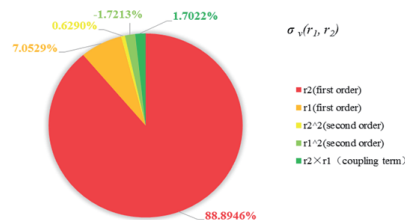


Fig. 18. Contribution rate in $\sigma_v(r_1, r_2)$

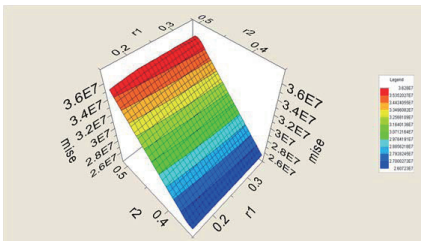


Fig. 19. Fitted design space of $\sigma_v(r_1, r_2)$

The design space of u shows as Fig. 17.

As Fig. 18, the rate of the couple term is 1.7022% to σ_v of airbeam. It's smaller but not ignorable, which in the same level with the second order in r_1 and r_2 . The design space of σ_v shows as Fig. 19.

Consequently, the influence caused by coupling term in r_1 and r_2 should be taken into consideration during tensairity girder design.

6. Conclusion

In term of tensairity girder design and optimization, a VCM optimization architecture based on nonlinear FEA and Kriging approximate method was constructed, which combined global optima explore with local optima seeking. A surrogate model based on Kriging method and updated by adaptive sampling method was built. In result, a high performance tensairity girder was produced by the optimization architecture. What's more, the quantitative analysis of sensitivity reveals the trend of responses with variables. The optimization architecture gives a reasonable design and optimization case for portable tensairity girder, the result approves the feasibility as well. In future work, the tender cable twined around the airbeam and stiff upper chord can be added to compose a whole tensairity for analysis and optimization.

References

- [1] Freeland, R. E., Bilyeu, G. D., Veal, G. R., Steiner, M. D. and Carson, D. E., "Large inflatable deployable antenna flight experiment results", *Acta Astronautica*, Vol. 41, No. 4, 1997, pp. 267-277.
DOI:10.1016/s0094-5765(98)00057-5
- [2] Lichodziejewski, D., Derbes, B., Slade, K., Mann, T. and Reinert, R., "Vacuum deployment and testing of a 4-quadrant scalable inflatable rigidizable solar sail system", *AIAA Paper* 3927, 2005.
DOI:10.2514/6.2005-3927
- [3] Yu, D. and Lv, X., "Configurations analysis for high-altitude/long-endurance airships", *Aircraft Engineering and Aerospace Technology*, Vol. 82, No. 1, 2010, pp. 48-59.
DOI:10.1108/00022661011028119
- [4] Elsley, G. H. and Devereux, A. J., *Hovercraft design and construction*, Cornell Maritime Press, 1968.
- [5] Luchsinger, R. H., Sydow, A. and Crettol, R., "Structural behavior of asymmetric spindle-shaped Tensairity girders under bending loads", *Thin-Walled Structures*, Vol. 49, No. 9,

2011, pp. 1045-1053.

DOI:10.1016/j.tws.2011.03.012

[6] LUCHSINGER, R. H. and TEUTSCH, U., "An analytical model for Tensairity girders", *Symposium of the International Association for Shell and Spatial Structures (50th. 2009. Valencia). Evolution and Trends in Design, Analysis and Construction of Shell and Spatial Structures: Proceedings. Editorial Universitat Politècnica de València*, 2009.

[7] Luchsinger, R. H., Pedretti, A., Steingruber, P. and Pedretti, M., "The new structural concept Tensairity: Basic principles", *Progress in structural engineering, mechanics and computation*, 2004, pp. 323-328.

[8] Cao Zhenggang, et al. "Basic mechanical behavior of spindle Tensairity structures", *China civil engineering journal*, Vol. 44, No. 1, 2011, pp. 11-18.

[9] Liang, H., Liang, H., Zhu, M. and Guo, X., "Multidisciplinary design optimization of composite wing by parametric modeling", *Proceedings of the 2013 International Conference on Mechatronic Sciences, Electric Engineering and Computer (MEC)*, IEEE, Shenyang, China, 2013.

DOI:10.1109/mec.2013.6885527

[10] Chen, X., Luo, W. and Zhang, W., *Research on the Theory and Application of Multidisciplinary Design Optimization of Flight Vehicles*, National defence of Industry Press, 2006

DOI: 10.2514/6.2006-1721

[11] Kaufman, M., Balabanov, V., Burgee, S. L., Giunta, A. A., Grossman, B., Haftka, R. T., Mason, W. H. and Watson, L. T., "Variable-complexity response surface approximations for wing structural weight in HSCT design", *Computational Mechanics*, Vol. 18, No. 2, 1996, pp. 112-126.

DOI: 10.2514/6.1996-89

[12] Zhang, X., *The basic mechanical property of tensairity [D]*. Diss. Harbin Institute of Technology, 2009.

[13] Hutchison, M. G., Mason, W. H., Grossman, B.

and Haftka, R. T., "Aerodynamic optimization of an HSCT configuration using variable-complexity modeling", *AIAA Paper 93-0101*, 1993.

DOI: 10.2514/6.1993-101

[14] Jeong, S., Murayama, M. and Yamamoto, K., "Efficient optimization design method using kriging model", *Journal of aircraft*, Vol. 42, No. 2, 2005, pp. 413-420.

DOI: 10.2514/1.17383

[15] Simpson, T. W., "Comparison of response surface and kriging models in the multidisciplinary design of an aerospike nozzle", 1998.

DOI: 10.2514/6.1998-4755

[16] Ooka, R. and Komamura, K., "Optimal design method for building energy systems using genetic algorithms", *Building and Environment*, Vol. 44, No. 7, 2009, pp. 1538-1544.

DOI: 10.1016/j.buildenv.2008.07.006

[17] Rubio-Solar, M., Vega-Rodríguez, M. A., Pérez, J. M. S., Gómez-Iglesias, A. and Cárdenas-Montes, M., "A FPGA optimization tool based on a multi-island genetic algorithm distributed over grid environments", *Cluster Computing and the Grid, 2008. CCGRID'08. 8th IEEE International Symposium on*. IEEE, 2008.

DOI: 10.1109/ccgrid.2008.96

[18] Lawrence, C. T. and Tits, A. L., "A computationally efficient feasible sequential quadratic programming algorithm", *Siam Journal on optimization*, Vol. 11, No. 4, 2001, pp. 1092-1118.

DOI: 10.1137/s1052623498344562

[19] Jiangxin, L. Y. and Liqiao, F., "Isight parameter optimization and application", 2012, pp. 144-156.

[20] YU, X. Q., YAO, W. X., XUE, F., MU, X. F., LIU, K. L. and HUANG, A. F., "A study on the Requirements for the Framework of Multidisciplinary Design Optimization", *Mechanical science and technology*, Vol. 23, No. 3, 2004, pp. 286-289.